17th International Drying Symposium (IDS 2010)
Magdeburg, Germany, 3-6 October 2010

SINGLE DROPLET EXPERIMENTATION ON SPRAY DRYING: EVAPORATION OF SESSILE DROPLETS DEPOSITED ON A FLAT SURFACE

J. Perdana[1], M. Fox[2], M.A.I Schutyser[1], R.M. Boom[1]

[1]*Food Process Engineering Group, Wageningen UR*
P.O. Box 8129, 6700 EV Wageningen, The Netherlands
Tel.:+31 31 7483435, E-mail: jimmy.perdana@wur.nl

[2]*NIZO Food Research*
P.O. Box 20, 6710 BA Ede, The Netherlands
Tel.:+ 31 318 659 513, E-mail: martijn.fox@nizo.nl

Abstract: Individually dispensed droplets were dried on a flat surface to mimic the drying of single droplets during spray drying. A robust dispensing process is presented that generates small droplets (d_p>150 μm). A predictive model based on Bernoulli's law accurately describes droplet size with varying liquids and dispensing parameters. Shrinkage of the droplets, monitored with a camera, was described using mass balance equations. Finally, a Sherwood correlation was derived to describe the mass transfer coefficient for sessile droplets. This work forms the basis for the development of a platform for high throughput experimentation on spray drying.

Keywords: spray drying, sessile droplet, fluid dispensing, Sherwood correlation

INTRODUCTION

Spray drying has a long history in food processing and other areas of industrial production. For more than 30 years, spray drying is the most common method to dehydrate for example milk products (Pierre 2002). Nowadays, spray drying is widely used for manufacturing e.g. milk powder, whey powder, baby food, lactose powder, and maltodextrin due to its advantages as stated by Filkova (1995):

1. Properties of the powder can be effectively controlled.
2. Spray drying allows high production capacity in continuous operation.
3. Heat-sensitive foods, biological products and pharmaceuticals can be dehydrated under relatively mild drying conditions.

Although spray drying is well established, it is difficult to find the optimal drying conditions for a given product. Numerous process parameters and feed properties during spray drying have an influence on final product quality and process efficiency. To avoid upscaling issues, it is necessary to carry out trials in representative pilot-scale spray dryers. These trials are costly and increase the time to market. Other disadvantages of existing spray dryers are the given design and operational parameters, e.g. operating temperatures, residence time, and liquid feed viscosity (have to be within certain limits), which makes it difficult to discover new windows of operation in combination with the development of new products.

Recently, researchers have attempted to scale down the experimental conditions from pilot-scale to as small as a single droplet (Brask et al. 2007; Schiffter and Lee 2007). Major advantage of this approach is the reduction of the number of pilot-scale tests. Drying of single droplets was for example assessed by using acoustic levitation to suspend a free droplet in the air. From imaging the shrinking droplets, it was possible to determine the drying kinetics at different drying conditions (Brask et al. 2007). In the current study we aim at the drying of single droplet dispensed on a flat surface. Advantages of the proposed approach is that multiple droplets can be dried simultaneous, residence time can be varied, and particles can be collected for further analysis (e.g. to monitor survival of bacteria after drying). In this study a robust dispensing method is investigated to produce a small initial droplet size of various liquids. The properties of the surface (on which the droplets are deposited) should be selected such that the droplets will retain their spherical shape, but do not move by the applied air flow. In this way the difference in drying behavior between a sessile and a free falling droplet is minimized. Finally, the drying behavior of the sessile droplets should be mapped to compare their drying behavior to that of droplets during spray drying.

AIM

The aim of this project is the development of a single droplet drying approach (based on the drying of a droplet deposited on a flat surface) that mimics drying of a droplet during spray drying.

MATERIALS AND METHODS

The experimental set-up is schematically shown in Fig. 2 and consists of the following units:

1. Micro-dispenser
2. Drying chamber
3. Camera system

The micro-dispenser was a Microdot 741MD-SS Dispense Valve [EFD]. Nitrogen (6 barg) was used to operate the micro-dispenser. As shown in Figure 2, a static pressure is applied to the fluid in the cylindrical fluid reservoir. The needle valve or piston opening time is controlled by the actuating pressure. When the valve is opened, liquid is dispensed through the needle tip. The standard needle diameter used in this study was 0.12 mm. An Ultra TT positioning system (EFD) was used to automate the dispensing process and to position the dispensed droplets.

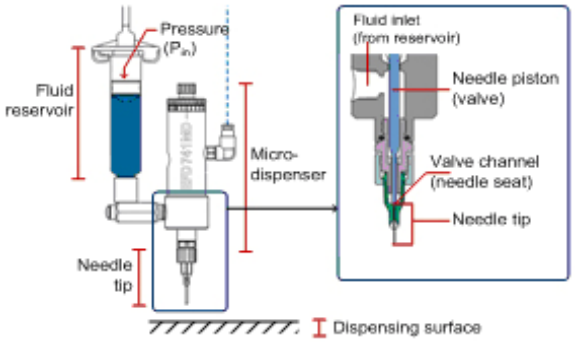

Fig. 1. Pneumatically driven micro-dispenser

To evaluate the micro-dispensing process, three different fluids were dispensed; monoethylene glycol (MEG), diethylene glycol (DEG), and polyethylene glycol 400 (PEG). Analytical grade solutions manufactured by Merck were used. Distilled water was dispensed for the drying experiments.

As shown in Fig. 3, the preconditioning of the drying air was carried out with two heat exchangers and a packed bubble column. The dry air stream was then split into two streams of which the flow rates were measured and controlled independently. The first stream was saturated with water in a packed bubble column (A). The second stream was passed through a heat exchanger to increase the air temperature to a set value. Both streams were then mixed and led through the second heat exchanger (B). Thus, the first heat exchanger was used to control the humidity of the air and the second heat exchanger was used to control the outlet air temperature.

Drying air was fed to the drying chamber via an insulated channel. In this channel, the air flow was developed while the temperature was maintained constant. The droplet was dispensed on the solid surface with the aid of the Ultra TT system. The position of the droplet sample was exactly in the center of the outlet of the channel.

The surface on which the droplets were deposited was a hydrophic membrane, i.e. Accurel® type PP 2E HF (Akzo Nobel Faser Ag.). For this membrane the water contact angle was determined to be 130^{O}.

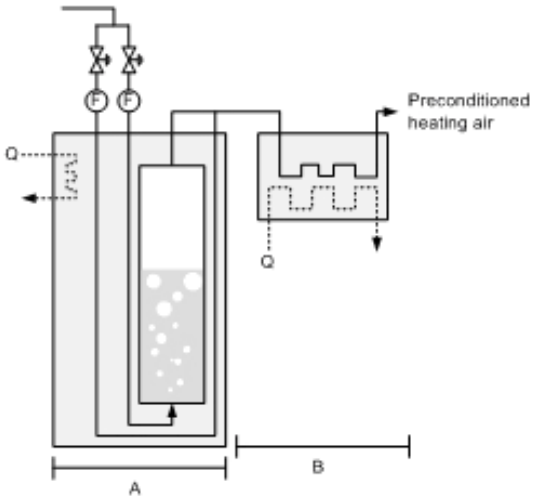

Fig. 3. Set-up for preconditioning of the drying air; consisting of a packed bubble column and a heat exchanger

The camera system consisted of a CCD camera (µEye 1480ME) with a magnification lens. The droplet was illuminated from the back using a

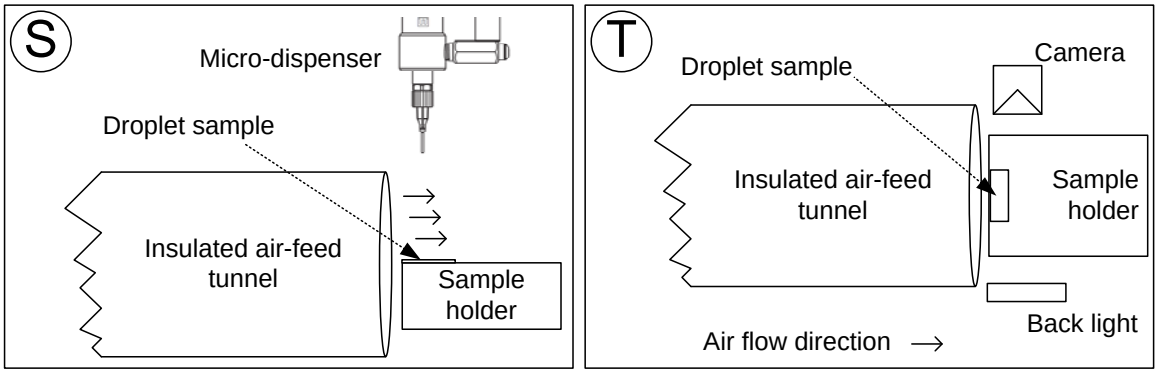

Fig. 2. Spray drying screening tool setup, side view (S) and top view (T)

diffused light (Lumimax SQ50-W).

THEORY

Micro-dispensing

The micro-dispensing process can be considered as a fluid flowing through a series of channels. To describe the micro-dispensing process, a model based on Bernoulli's law is proposed. Several assumptions and considerations were checked and found to hold:

- Newtonian flow behaviour of the dispensed fluids.
- The dispensing resistance is (>99%) dominated by the needle tip, which is the narrowest channel in the dispensing system (Darby 2001).
- The small increase in temperature (< 3 ^{o}C) has no significant effect on fluid viscosity.
- The Laplace pressure is less than 5% of the applied pressure for dispensing the smallest droplets and thus assumed negligible

For non-compressible fluids, Bernoulli's equation (Steffe and Singh 1997; Deplanque and Rangel 1998) can be written as:

$$\left(\frac{P_o - P_i}{\rho}\right) + g(z_o - z_i) + \frac{1}{2}\alpha\left(v_o^{\,2} - v_i^{\,2}\right) + w + e_f = 0 \quad (1)$$

which gives the energy per unit mass due to the applied pressure difference (first term), the potential energy difference (second term), the kinetic energy difference (third term), the shaft work (fourth term), and the friction in pipes and appendages (fifth term). The value of the kinetic energy correction factor (α) is taken 2, which is valid for laminar flow (Darby 2001). In the micro-dispenser, the needle piston movement to open and close the valve can be regarded as shaft work and determines the minimum dispensed fluid that can be achieved.

The total friction loss of the system is the summation of all frictions due to the length of the pipes, valves, fittings, contractions or expansions:

$$e_f = \sum_i \frac{K_{f_i} v_i^{\,2}}{2} \quad (2)$$

99% of the resistance to liquid flow is calculated to be present in the needle and the contraction between needle and needle chamber. The fanning friction factor (f) is determined for laminar flow, which depends on the Reynolds number, regardless the wall roughness. The friction coefficient (K_f) is described by:

$$K_f = 4f\frac{L}{d_h};\ f = \frac{16}{Re} \quad (3)$$

To predict the resistance to flow due to contraction between the needle and the needle chamber the following friction coefficient was proposed by Sylvester and Rosen (1970):

$$K_f = K + \frac{K'}{Re} \quad (4)$$

with K = 2.4 and K'= 295. This correlation is valid for a contraction factor ($d_{c,out}/d_{c,in}$) of 0.016 and 6<Re<2000, which is valid to the dispensing conditions in this study.

Equation 1 is numerically solved and yields the outlet fluid velocity (v_o) of the dispensed fluid. The droplet volume can then be calculated as follows:

$$V_d = v_o t_{dis} \quad (5)$$

Drying of a single sessile droplet

The evaporation of a single sessile droplet cannot be considered similar to that of an ideal spherical body because of the evolution in geometry during the drying. In Fig. 4 the evolution of a drying sessile droplet is sketched. It is found that during our drying experiments the wetted droplet surface ($2\cdot l_d$) remained constant. Thermodynamically, one would expect a constant contact angle. However, due to surface roughness a constant base diameter is often observed as well. This phenomenon is also known as contact angle hysteresis (Picknett and Bexon 1976). It is noted that during the drying of actual food suspensions (e.g. concentrated milk) the droplet height will only be reduced with approximately 30% and thus the final particle shape will not be completely flat.

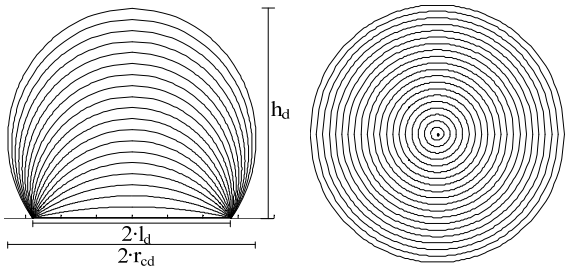

Fig. 4. Droplet evolution due to evaporation of a pure liquid; sessile droplet (left) and spherical body (right)

Drying of single droplets has been investigated in numerous studies, e.g. the work of Ranz-Marshall (1952). The mass transfer coefficient can be obtained from Sherwood correlations that describe the mass transfer coefficient as a function of hydrodynamic conditions and the geometry of the drying object. The general Sherwood correlation is the following (Oliveira and Oliveira 2003):

$$Sh = \frac{k_{ev} l_c}{D} = P_1 + P_2\, Re^{P3}\, Sc^{P4} \quad (6)$$

In which, the Reynolds and Schmidt numbers are defined as:

$$Re = \frac{\rho_a d_p v_a}{\mu_{gas}} \quad (7)$$

$$Sc = \frac{\mu_a}{\rho_a D} \quad (8)$$

In the field of spray drying the Sherwood correlation for a free falling spherical body is mostly applied. The Sherwood and Nusselt relations for heat and mass transfer for this case are:

$$Sh = \frac{k_{ev} l}{D} = 2.0 + 0.6\,Re^{1/2}\,Sc^{1/3} \quad (9)$$

$$Nu = \frac{h_c d_p}{k_a} = 2.0 + 0.6\,Re^{1/2}\,Pr^{1/3} \quad (10)$$

in which the Prandtl number is equal to:

$$Pr = \frac{cp_a \mu_a}{k_a} \quad (11)$$

In this study we focus on the drying of a droplet deposited on a flat surface. Baines and James (1994) indicate that the Sherwood correlation for a deposited droplet is comparable to that for flow across a flat plate:

$$Sh = 0.664\,Re^{1/2}\,Sc^{1/3}\ ;\ Sc > 0.6 \quad (12)$$

Evaporation of water from a sessile droplet is a coupled heat and mass transfer process (Sloth et al. 2006; Mezhericher et al. 2008). For a sessile droplet heat is partially transferred via the drying air and via the solid surface that is heated by the drying air. Therefore, the total heat balance is:

$$m_d c_{pl} \frac{dT}{dt} = U_{conv} A_{la} \Delta T_{la} + U_{cond} A_{ls} \Delta T_{ls} - \frac{dm_d}{dt} \Delta H_{vap} \quad (13)$$

in which ΔT_{la} is the temperature difference between the droplet and the air; and ΔT_{ls} is the temperature difference between the droplet and the solid surface. The exact temperature of the droplet was not determined during this study. For the calculations on mass transfer it was assumed that the drying occurred near the wet bulb temperature (Pisecký 1995).

The change in droplet mass during evaporation can be described as follows:

$$-\frac{dm_d}{dt} = -\rho_l \frac{dV_d}{dt} = k_{ev} A_{la} \frac{M_l}{R}\left(\frac{P_s}{T_s} - \frac{P_{ba}}{T_{ba}}\right) \quad (14)$$

in which P_s is the saturated vapour pressure at 26°C (the correlated wet bulb temperature of the drying air with temperature 80°C and relative humidity 0%) and P_{ba} is the vapour pressure of the drying air, which is taken zero.

The change in droplet volume can be related to the change in height:

$$dV_d = 2\pi r_{cd} \frac{h_d}{2} dh_d \quad (15)$$

in which r_{cd} is the radius curvature of the droplet.

$$r_{cd} = \frac{h_d^2 + l_d^2}{2h_d} \quad (16)$$

The contact area between the sessile droplet and the drying air (A_{la}) is given by:

$$A_{la} = \pi\left(h_d^2 + l_d^2\right) \quad (17)$$

Finally, the change in droplet height can then be described:

$$-\rho_l \frac{\frac{1}{2}\pi\left(h_d^2 + l_d^2\right)dh_d}{dt} = k_{ev}\pi\left(h_d^2 + l_d^2\right)\frac{M_l}{R}\left(\frac{P_s}{T_s} - \frac{P_{ba}}{T_{ba}}\right) \quad (18)$$

The equation above can be simplified to:

$$-\frac{dh}{dt} = 2\frac{k_{ev}}{\rho_l}\frac{M_l}{R}\left(\frac{P_s}{T_s} - \frac{P_{ba}}{T_{ba}}\right) \quad (19)$$

The mass transfer coefficient (k_{ev}) can be obtained by fitting Equation 19 to the experimental data.

RESULTS AND DISCUSSION

To systematically evaluate the micro-dispensing and the evaporation, the results are discussed separately.

Dispensing process

A pneumatic micro-dispenser is used to produce droplets of a size similar to the droplet size during spray drying. A robust dispenser was selected that can produce small droplets and at the same time dispense viscous liquids, which is a prerequisite for the dispensing of concentrated liquid foods. The micro-dispensing process is influenced by process parameters (valve opening time and applied pressure) and product properties (viscosity and rheological behavior).

The top view of the deposited droplets was visualized with a microscope. From the top view and the contact angle the droplet volume was calculated. The droplet volume is shown as a function of applied dispensing pressure and valve opening time in Fig. 5:

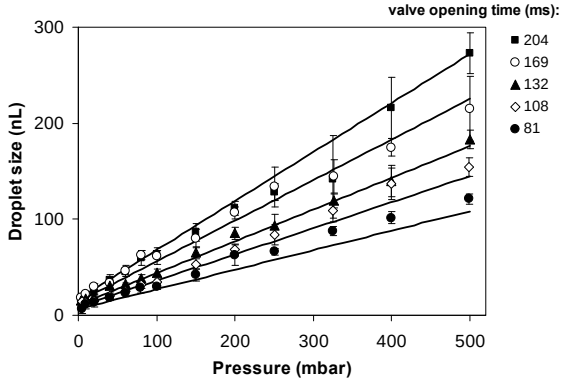

Fig. 5. Effect of dispensing pressure and valve opening time on MEG droplet volume. The symbols represent the experimental values. The lines represent the values predicted by the model based on Bernoulli's law

Fig. 5 shows that droplet volume increases with pressure and valve opening time. In practice, the smallest droplet that can be generated has a diameter of 150 μm (~2 nL). This minimum droplet size is influenced by the moving needle valve (in the micro-dispenser) during opening and closing. The experimental results are compared to the predicted droplet volume by a model based on Bernoulli's law (Equation 1). As shown in Fig. 5, the predicted droplet size is in close agreement with the experimental data.

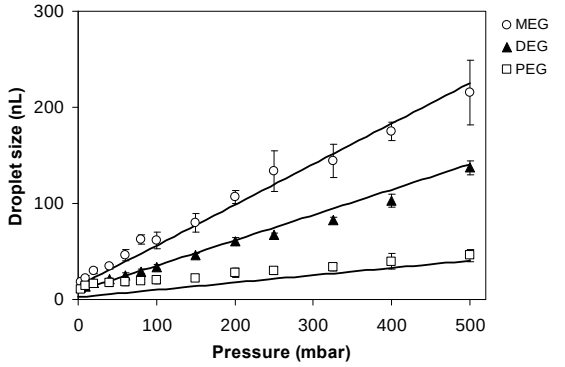

Fig. 6. Effect of fluid properties (viscosity) on droplet size (valve opening time = 169.3 ms)

The viscosities of MEG, DEG, and PEG-400 at 30^{O}C are 13, 21, and 71 mPa.s, respectively. Rheology experiments show that the fluids exhibit Newtonian behavior in the range of shear rates applied. Fig. 6 shows that droplet size decreases with increasing fluid viscosity. Bernoulli's law also includes the effect of viscosity on dispensed droplet size. As shown in Fig. 6, the predictions are in good agreement with the experimental data.

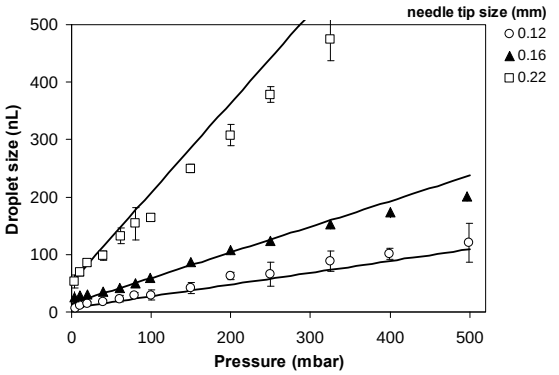

Fig. 7. Effect of needle tip size on MEG dispensed volume (valve opening time = 81.5 ms)

Three different sizes of needle tips were used; 27 gauge (0.22 mm), 30 gauge (0.16 mm), and 32 gauge (0.12 mm). As shown in Fig. 7, the model was in agreement with the experimental data. From these results, it is concluded that Bernoulli's law can account for the effects of applied pressure, valve opening time, needle tip size, and fluid viscosity on droplet size. Thus, if the liquid viscosity is known and an appropriate needle tip size is chosen, the pressure and valve opening time can be controlled to deposit the required droplet size.

Drying process

The evaporation of a single dispensed droplet was investigated as a function of the drying air conditions. The effect of the slip velocity between the droplet and drying air on the drying of a sessile water droplet is investigated here. In Fig. 8, snapshots of a droplet are shown during the drying process.

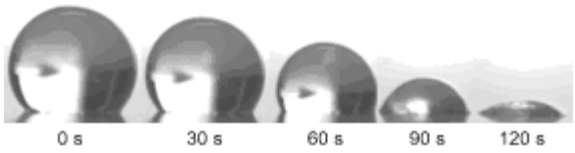

Fig. 8 Snapshots of a shrinking droplet, drying at a constant drying air velocity of 0.30 m/s (T = 80^{O}C, RH ~ 0%)

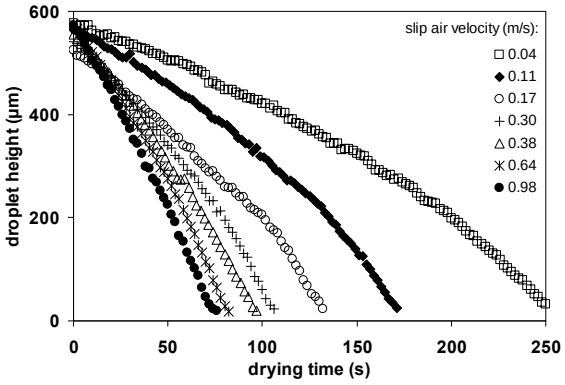

Fig. 9. Droplet height as a function of drying time at different slip air velocities

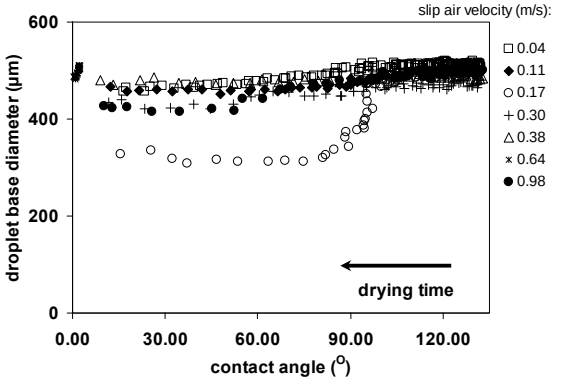

Fig. 10. Droplet base diameter as function of the contact angle during the drying process

Fig. 8, Fig. 9, and Fig. 10 show that the droplet geometry evolves mainly in height, while the contact area between droplet and the flat surface (base diameter) remains constant. This finding is in agreement with the observations of Hu and Larson (2002) who observed that the contact angle of water droplets deposited on a glass surface changed from 40^{O} to a minimum contact angle of 2–4^{O}, while the base diameter remained constant. In the current study similar observations were obtained; the droplet base diameter tends to be constant during drying (Fig. 10). It was observed that during the drying experiment with the air slip velocity of 0.17 m/s, the droplet base diameter suddenly changed. Possibly, this is due to an irregularity in the microscopic surface of the membrane. After the sudden change in the droplet base diameter, it remains constant again with changing contact angle.

The experimental data on the change in height may be compared to Equation 19. A characteristic length is used for the calculations of the Sherwood and Reynolds number. The characteristic length (l_c) is defined as:

$$l_c = \frac{\text{object surface area}}{\text{perpendicular object perimeter}}$$

For sessile droplets, the characteristic length is:

$$l_c = \frac{A}{P} = \frac{\pi h}{\theta} \qquad (20)$$

The mass transfer coefficient (k_{ev}) for a free spherical droplet is calculated using the Sherwood number from the Ranz-Marshall correlation (Equation 9). The mass transfer coefficient is then used to describe the height as a function of the drying time using Equation 19. The results are shown in Fig. 11.

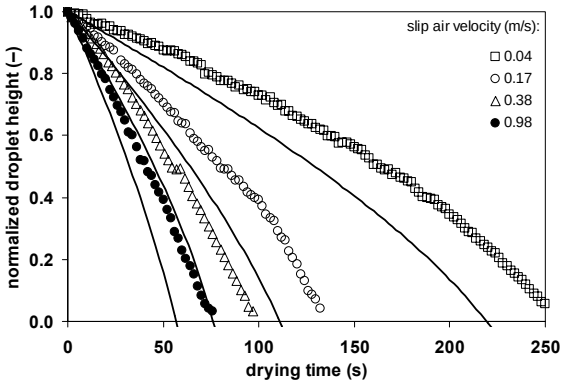

Fig. 11. Normalized droplet height as a function of the drying time at different slip air velocities; the solid line represents the model in which the particle is a free falling sphere (Ranz-Marshall correlation)

Fig. 11 shows that the height of a free droplet decreases faster than that of a sessile droplet. It is concluded that the drying of the sessile droplet, even when with a high contact angle (130^{o}), cannot be approximated by directly using the mass transfer coefficient for a free spherical droplet. Therefore, a specific Sherwood correlation was determined for the drying of a sessile droplet by fitting the parameters of the general Sherwood correlation (Equation 6) to the experimental data.

Vapour-air diffusivity and air viscosity were taken at the wet bulb temperature of 26^{o}C and assumed constant in the experiments. The Schmidt number is thus constant in this study, i.e. 0.62. Therefore, it was not possible to estimate the power of the Schmidt number.

The estimated Sherwood correlation are shown in Table 1 and compared to the values from literature for several cases. The parameter values for the Sherwood correlation (Equation 6) in this study were obtained by fitting the predictive model (Equation 19) to the experimental height data as shown in Fig. 12.

Table 1 Estimated parameter values for the general Sherwood correlation for different cases

$Sh = P_1 + P_2 Sc^{P4} Re^{P3}$			
P_1	$P_2 Sc^{P4}$	P_3	Case

0.24	0.53	0.51	Sessile droplet, initial contact angle 130^o This work
2.0	0.51	0.50	Free sphere Ranz-Marshall (1952)
0	0.56	0.50	Laminar flow across flat plate (Oliveira and Oliveira 2003); Sc>0.6

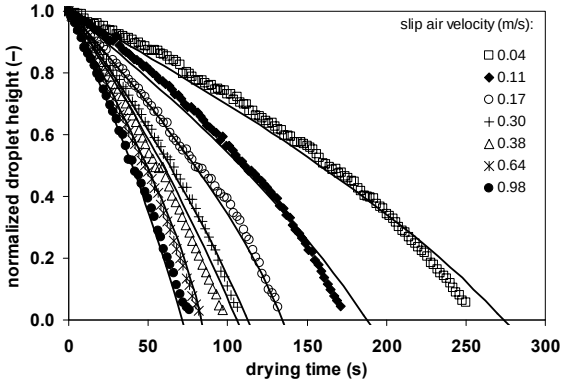

Fig. 12. Comparison between the estimated Sherwood correlation (solid line) and the experimental data (points)

Table 1 shows that the estimated parameter values in this study are different compared to those of the flat plate and the falling sphere. Specifically, the parameter value P_1 is found to be in between the two cases. The value of P_1 reflects the limiting Sherwood value where diffusional mass transfer occurs predominantly. The value of P_1 is 2.0 for a spherical object and 0 for a flat object. The sessile droplet changes from a nearly spherical to a flat object, which is reflected in a decreasing contact angle. The value of P_1 (0.24) in this study is only valid for a sessile droplet with an initial contact angle of 130^o that decreases to nearly 0^o. More information about the effect of contact angle on the Sherwood number for the diffusional regime can be found in literature (Baines and James, (1994). It is expected that the P_1 value for drying of a droplet from a suspension will be higher if the droplet will only partially evaporate. Furthermore, to better mimic the drying behavior of a free falling droplet it is suggested to for example micro-fabricate a 'hairy' surface structure that is better able to retain the spherical shape of the drying droplet (i.e. making use of the Lotus effect).

The estimated value of P_2 for this work is 0.62, if it is assumed that P_4 is 1/3 (a common value for the power of the Schmidt number). For a free falling sphere P_2 is found equal to 0.60 and for a flat surface equal to 0.67. The value of the estimated parameter P_3 in this study (0.51) is comparable to the P_3 values in the Sherwood correlations for flow across a flat surface and a falling sphere.

CONCLUSIONS

The dispensing of liquid droplets was carried out with a pneumatic dispenser and could be controlled accurately by varying applied pressure and valve opening time. A predictive model based on Bernoulli's law was developed and compared to experimental data. Good agreement was found between dispensed and predicted droplet volume.

Drying of single sessile water droplets was experimentally monitored with a camera set-up. Drying was assumed to occur at the wet bulb temperature. Experimental data of the shrinking droplets were compared with a predictive model based on mass transfer for a single free falling sphere. It was found that the Sherwood correlation of a free falling sphere did not predict the appropriate mass transfer coefficient for the drying sessile droplet. Therefore, a Sherwood correlation was derived for the drying of sessile water droplets: $\mathrm{Sh} = 0.24 + 0.62\,\mathrm{Re}^{0.51}\,\mathrm{Sc}^{1/3}$ for Sc=0.62. This correlation was found almost similar to the Sherwood correlation for flow across a flat surface and a free falling sphere except for the value of P_1. It is expected that this value will increase when drying food suspensions or when a micro-fabricated 'hairy' surface structure is used.

It is planned to further investigate the drying of complex solutions, i.e. food products, which are highly viscous or contain specific heat sensitive ingredients. During drying of these products, the temperature of the product will start deviating from the wet bulb temperature. Furthermore, a challenge will be the subsequent analysis of very small particles. Therefore, it is intended to develop the platform into a high throughput experimentation system to dry multiple droplets at the same time.

NOMENCLATURE

A	surface area	m^2
c_p	specific heat capacity at constant pressure	$J.kg^{-1}.K^{-1}$
d	diameter	m
D	diffusion coefficient	m^2s^{-1}
e_f	friction loss per unit mass	$N.m.kg^{-1}$
f	fanning friction factor	–
g	acceleration gravity constant	$m.s^{-2}$
h_c	convective heat transfer coefficient	$W.m^{-2}K^{-1}$
h_d	Droplet height	m
ΔH_{vap}	enthalpy of vaporization	$J.kg^{-1}$
k	thermal conductivity	$W.m^{-1}K^{-1}$
k_{ev}	Convective mass transfer coefficient	$m.s^{-1}$
K	Hagenbach-Couette correction factor for narrow gap contraction	–
K'	Hagenbach-Couette	–

	correction factor for narrow gap contraction	
K_f	friction loss coefficient	–
l_c	characteristic length in Sherwood number	m
l_d	Droplet base radius	m
L	Channel length	m
m	mass	kg
M	Molecular weight	$kg.mol^{-1}$
Nu	Nusselt number	
P	pressure	Pa
Pr	Prandlt number	–
r_c	radius curvature	m
Re	Reynolds number	–
Sc	Schmidt number	–
Sh	Sherwood number	–
t	time	s
T	temperature	^{O}C or K
U	Overall heat transfer coefficient	$W.m^{-2}K^{-1}$
v	velocity	$m.s^{-1}$
V	volume	m^3
w	shaft work in micro-dispenser per unit mass	$N.m.kg^{-1}$
x	length coordinate	m
z	height coordinate	m

Greek letters

α	Kinetic energy correction factor	–
Δ	Difference	–
μ	dynamic viscosity	$kg.m^{-1}.s^{-1}$
π	pi value; 3.14	
θ	Contact angle	rad
ρ	density	$kg.m^{-3}$

Subscripts

a	Air
ba	Bulk air
conv	Convection
cond	Conduction
d	Droplet
dis	Dispensing
i	In
l	Liquid, i.e. water
o	Out
p	Particle
s	Solid

ACKNOWLEDGEMENTS

We thank Advanced Chemical Technologies for Sustainability (ACTS)–Netherlands Organization for Scientific Research (NWO) for financial aid through Process on a Chip (PoaC) program.

REFERENCES

Baines, W. D. and D. F. James (1994). "Evaporation of a droplet on a surface." Industrial & Engineering Chemistry Research 33(2): 411-416.

Brask, A., et al. (2007). "High-Temperature Ultrasonic Levitator for Investigating Drying Kinetics of Single Droplets." Niro A/S.

Darby, R. (2001). Chemical Engineering Fluid Mechanics. New York, Marcel Dekker, Inc.

Deplanque, J. P. and R. H. Rangel (1998). "A comparison of models, numerical simulation, and experimental results in droplet deposition processes." Acta Materialia 46(14): 4925-4933.

Filkova, I. and A. S. Mujumdar (1995). Industrial Spray Drying System. Handbook of Industrual Drying. A. S. Mujumdar. New York Marcel Dekker, Inc.

Hu, H. and R. G. Larson (2002). "Evaporation of a Sessile Droplet on a Substrate." The Journal of Physical Chemistry B 106(6): 1334-1344.

Mezhericher, M., et al. (2008). "Heat and mass transfer of single droplet/wet particle drying." Chemical Engineering Science 63(1): 12-23.

Oliveira, F. A. R. and J. C. Oliveira (2003). Sherwood Number, Taylor & Francis: 895-901.

Picknett, R. G. and R. Bexon (1976). "The Evaporation of Sessile or Pendant Drops in Still Air." Journal of Colloid and Interface Science 61(2): 336-350.

Pierre, S. (2002). "Spray drying of dairy products: state of the art." Le Lait 82(4): 375-382.

Pisecký, J. (1995). Evaporation and Spray Drying in the Dairy Industry Handbook of Industrial Drying: Volume 1. A. S. Mujumdar. Boca Raton, CRC Press.

Ranz, W. E. and W. R. Marshall (1952). "Evaporation from Drops." Chemical Engineering Progress 48: 141-146; 173-180.

Schiffter, H. and G. Lee (2007). "Single-droplet evaporation kinetics and particle formation in an acoustic levitator. Part 1: Evaporation of water microdroplets assessed using boundary-layer and acoustic levitation theories." Journal of Pharmaceutical Sciences 96(9): 2274-2283.

Sloth, J., et al. (2006). "Model based analysis of the drying of a single solution droplet in an ultrasonic levitator." Chemical Engineering Science 61(8): 2701-2709.

Steffe, J. F. and R. P. Singh (1997). Pipeline Design Calculations for Newtonian and Non-

Newtonian Fluids. Handbook of Food Engineering Practice, CRC Press.

Sylvester, N. D. and S. L. Rosen (1970). "Laminar flow in the entrance region of a cylindrical tube: Part I. Newtonian fluids." AIChE Journal 16(6): 964-966.